




Glass formation and properties of Ti-based bulk metallic glasses as potential biomaterials with Nb additions

Hui-Ming Yan, Ying Liu, Shu-Jie Pang* ,
Tao Zhang

Received: 24 October 2014/Revised: 21 December 2014/Accepted: 13 November 2015/Published online: 19 December 2015
© The Nonferrous Metals Society of China and Springer-Verlag Berlin Heidelberg 2015

Abstract $\text{Ti}_{47}\text{Cu}_{38-x}\text{Zr}_{7.5}\text{Fe}_{2.5}\text{Sn}_2\text{Si}_1\text{Ag}_2\text{Nb}_x$ ($x = 0, 1, 2$; at%) bulk metallic glasses (BMGs) with superior bio-corrosion resistance were synthesized by copper mold casting. Although the minor addition of Nb to the Ti–Cu–Zr–Fe–Sn–Si–Ag BMG slightly decreases the glass-forming ability (GFA), the Nb-bearing Ti-based alloys could be casted in a bulk glassy rod form with diameters up to 3 mm. It is found that partial substitution of Cu with Nb is effective on enhancing the bio-corrosion resistance of the Ti-based BMG. Potentiodynamic polarization measurements show that Nb addition to Ti-based BMG leads to higher open-circuit potential and pitting potential as well as lower passive current density in Hank's solution. Electrochemical impedance spectroscopy (EIS) results indicate that with Nb content increasing, the charge transfer resistance values of the Ti-based BMGs become larger, demonstrating that the surface oxide films are more protective. The Nb-bearing Ti-based BMGs also exhibit good in vitro biocompatibility comparable to that of Ti–6Al–4V alloy. The enhanced bio-corrosion resistance, excellent in vitro biocompatibility and good mechanical properties of the Nb-bearing Ti-based BMGs are favorable for biomedical applications.

Keywords Ti-based alloy; Bulk metallic glass; Bio-corrosion; Electrochemical impedance spectroscopy; Biocompatibility

1 Introduction

Ti-based bulk metallic glasses (BMGs) with high yield strength, low Young's modulus, high bio-corrosion resistance as well as good formability have potential to be used as biomaterials [1–9]. Considering the biocompatibility, Ti-based BMGs free from highly toxic elements, such as Ni and Be which are the usual constituent components of Ti-based alloy for achieving high glass-forming ability, are desired. Recently, Pang et al. [4] have succeeded in synthesizing a novel Ni- and Be-free $\text{Ti}_{47}\text{Cu}_{38}\text{Zr}_{7.5}\text{Fe}_{2.5}\text{Sn}_2\text{Si}_1\text{Ag}_2$ BMG with critical diameter up to 7 mm by tilt copper mold casting, and the glassy alloy possesses good mechanical properties, high bio-corrosion resistance and excellent in vitro biocompatibility, demonstrating the application potential as an implant material. Potentiodynamic polarization indicated that the Ti–Cu–Zr–Fe–Sn–Si–Ag BMG was spontaneously passivated with low passive current density in phosphate-buffered saline (PBS) solution, while pitting corrosion occurred at relatively high potential [4].

It is known that when implanted into human bodies, metallic materials are usually subjected to corrosive processes once they get in touch with the aggressive physiological environment, which comprises amino acids, organic acids, proteins and many inorganic ions such as chlorine [10, 11]. Metal ions released from corrodible metal biomaterials to the surrounding tissues in human bodies will cause adverse biological responses, leading to clinical implant failures [11]. Meanwhile, the release of ions will also adversely affect the mechanical properties and biocompatibility, thus decreasing the service life of the implanted metallic materials. Therefore, further improving the bio-corrosion resistance, especially the pitting corrosion resistance, is of great importance for the biomedical

H.-M. Yan, Y. Liu, S.-J. Pang*, T. Zhang
Key Laboratory of Aerospace Materials and Performance
(Ministry of Education), School of Materials Science and
Engineering, Beihang University, Beijing 100191, China
e-mail: pangshujie@buaa.edu.cn

application of the Ti–Cu–Zr–Fe–Sn–Si–Ag BMG. It has been demonstrated that adding strongly passivating Nb element into Ti-, Zr- and Cu-based BMGs is an effect way to improve the corrosion resistance, especially the pitting corrosion resistance [5, 12–17]. On the other hand, among the constituent elements of the Ti–Cu–Zr–Fe–Sn–Si–Ag BMG, Cu is a relatively unstable element in the solutions containing chloride ions [16, 17]. Nb is also recognized as a much more favorable element with respect to Cu from the viewpoint of biocompatibility [7].

Therefore, in this work, addition of Nb to the Ti–Cu–Zr–Fe–Sn–Si–Ag BMG for replacing partial of Cu was conducted in order to further enhance the bio-corrosion resistance, and the effects of Nb-minor alloying on glass-forming ability (GFA), thermal properties, bio-corrosion behaviors in Hank's solution, in vitro biocompatibility and mechanical properties of the Ti-based BMG were investigated. The mechanisms of the glass formation and bio-corrosion behavior were also discussed.

2 Experimental

Alloy ingots with nominal compositions of $\text{Ti}_{47}\text{Cu}_{38-x}\text{Zr}_{7.5}\text{Fe}_{2.5}\text{Sn}_2\text{Si}_1\text{Ag}_2\text{Nb}_x$ ($x = 0, 1, 2$; at%) were prepared from the pure elements by arc melting in a Ti-gettered high-purity argon atmosphere. The mixture of pure Ti and Nb metals was firstly melted to form a pre-alloy and then remelted with the other constituent elements. Ribbon samples and cylindrical rod samples with different diameters were prepared from the master alloys by melt spinning and injection copper mold casting in an argon atmosphere, respectively. Microstructure of the samples was examined by X-ray diffraction (XRD, Bruker AXS D8) using Cu $K\alpha$ radiation. Thermal behavior of the samples was evaluated using differential scanning calorimeter (DSC, Netzsch 404 °C) at a heating rate of $0.33 \text{ K}\cdot\text{s}^{-1}$.

Bio-corrosion behaviors of the glassy alloys in Hank's solution at about 310 K were characterized by electrochemical measurements. Prior to the corrosion measurements, the surface of each ribbon sample was mechanically polished with silicon carbide paper up to 2000-grit in cyclohexane, degreased in acetone, washed in distilled water, dried in air and further exposed to air for about 24 h for good reproducibility. For simulating the human body environment, before the electrochemical measurements, the Hank's solution was heated to 310 K with a water bath and aerated with 4 vol% O_2/N_2 mixed gas at a flowing rate of $50 \text{ ml}\cdot\text{min}^{-1}$, which was continued throughout the measurements. Electrochemical measurements were conducted in a three-electrode cell using a platinum counter electrode and a saturated calomel reference electrode

(SCE). Potentiodynamic polarization was measured at a potential sweep rate of $0.833 \times 10^{-3} \text{ V}\cdot\text{s}^{-1}$ after open-circuit immersion for about 1800 s when the open-circuit potential (OCP) became almost steady. Electrochemical impedance spectroscopy (EIS) measurement was also carried out at the OCP with an alternating current (AC) amplitude of $\pm 5 \text{ mV}$ in the frequency ranging from 1×10^{-2} to $1 \times 10^4 \text{ Hz}$. The impedance data were interpreted on the basis of equivalent circuit, using the ZSimpWin software for fitting the experimental data. For each electrochemical measurement, at least three samples of each alloy were used to confirm the reproducibility.

MC3T3-E1 osteoblast cell line was adopted for preliminary evaluating the in vitro biocompatibility of the Nb-bearing Ti-based BMGs in comparison with the Ti–6Al–4V alloy. Cell culture was performed simultaneously on six samples of each alloy. All the samples with a size of $\Phi 3.0 \text{ mm} \times 1.5 \text{ mm}$ were mechanically polished with ascending grades of silicon carbide paper up to 2000-grit, followed by polishing to achieve a mirror-like finish. Subsequently, the samples were ultrasonically cleaned in acetone, ethanol and distilled water for 10 min, respectively. Each side of the substrates was sterilized for 1 h by exposure to ultraviolet–visible (UV-Vis) light. MC3T3-E1 osteoblast cells were firstly seeded at a cell density of $4 \times 10^4 \text{ cell}\cdot\text{ml}^{-1}$ per well on the prepared substrates in a 96-well plate, then cultured in alpha minimum essential medium (α -MEM), and supplemented with 10 % fetal bovine serum and 1 % antibiotic (penicillin) in a 5 vol% CO_2 balanced air at 310 K. The potential cytotoxicity of the Ti-based BMGs and Ti–6Al–4V alloy was evaluated by 3-(4,5-dimethyl-2-thiazolyl)-2,5-diphenyl-2-H-tetrazolium bromide (MTT) assay, and three samples of each alloy were evaluated for reproducibility. After incubation for 24 h, the medium was replaced with 100 μl α -MEM and 25 μl MTT in each well and incubated at 310 K for 4 h. The absorbance of the supernatants was measured by a microplate reader at 492 nm. The cell morphology on the remaining three samples of each alloy was observed by scanning electron microscope (SEM, JEOL JSM-6010LA) after cultivating for 24 h.

Compressive mechanical properties of the Ti-based BMGs were evaluated on a material testing machine at a strain rate of $2.0 \times 10^{-4} \text{ s}^{-1}$, and the samples were 2 mm in diameter and 4 mm in length. At least three samples were tested to ensure the repeatability of the results. Morphologies of the deformed samples were observed by scanning electron microscope (SEM). Young's modulus (E) was determined using ultrasound velocity measurement [18]. Microhardness of the glassy alloys was measured by Vickers hardness tester under the load of 1.96 N. Densities of the Ti-based alloys were measured by the Archimedeian method.

3 Results and discussion

XRD patterns of the as-cast $\text{Ti}_{47}\text{Cu}_{38-x}\text{Zr}_{7.5}\text{Fe}_{2.5}\text{Sn}_2\text{Si}_1\text{Ag}_2\text{Nb}_x$ rods with critical diameter of 3 mm prepared by injection copper mold casting are shown in Fig. 1. The XRD patterns exhibit a characteristic of broad diffraction hump without any distinct crystalline peak, indicating the glassy structure. In previous work, it was found that the $\text{Ti}_{47}\text{Cu}_{38}\text{Zr}_{7.5}\text{Fe}_{2.5}\text{Sn}_2\text{Si}_1\text{Ag}_2$ BMG with a diameter of 5 mm could be formed by injection copper mold casting. This result indicates that the minor alloying of 1 at% Nb to the Ti-based alloy is slightly detrimental on glass formation, while the addition of more Nb up to 2 at% does not lead to a further reduction in the GFA. DSC curves of $\text{Ti}_{47}\text{Cu}_{38-x}\text{Zr}_{7.5}\text{Fe}_{2.5}\text{Sn}_2\text{Si}_1\text{Ag}_2\text{Nb}_x$ glassy rods with their critical diameters are shown in Fig. 2, where T_g and T_x denote glass transition temperature and the onset temperature of crystallization, respectively. It is seen that the Ti-based alloys exhibit the sequential transition of the distinct glass transition, supercooled liquid region and crystallization. The values of T_g , T_x and supercooled liquid region ($\Delta T_x = T_x - T_g$) for the alloys are summarized in Table 1. With Nb content increasing from 0 at% to 2 at%, T_g gradually increases from 640 to 654 K, whereas T_x exhibits no obvious change in the range of 693–695 K, leading to the decrease in supercooled liquid region from 54 to 40 K. The DSC traces of the melt-spun ribbon samples were also examined for comparison, and the result demonstrates that the values of T_g , T_x and heat release of crystallization are nearly identical for the ribbon and the rod samples with the same compositions, which further confirms the amorphous structure of the bulk alloys. The positive mixing heats of Nb–Ti, Nb–Zr and Nb–Cu atomic pairs are 2, 4 and 3 $\text{kJ}\cdot\text{mol}^{-1}$ [19], respectively; therefore, the addition of Nb to the Ti–Cu–Zr–Fe–Sn–Si–Ag BMG is unsatisfied with

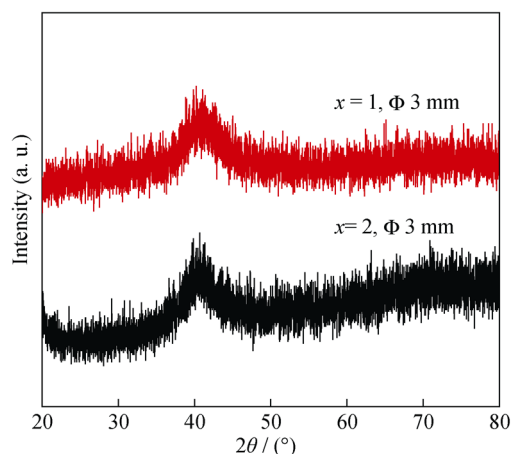


Fig. 1 XRD patterns of $\text{Ti}_{47}\text{Cu}_{38-x}\text{Zr}_{7.5}\text{Fe}_{2.5}\text{Sn}_2\text{Si}_1\text{Ag}_2\text{Nb}_x$ BMGs with their critical diameters prepared by injection copper mold casting

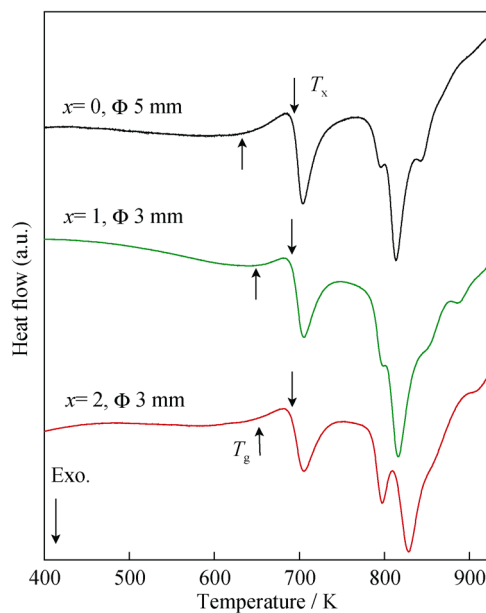


Fig. 2 DSC curves of $\text{Ti}_{47}\text{Cu}_{38-x}\text{Zr}_{7.5}\text{Fe}_{2.5}\text{Sn}_2\text{Si}_1\text{Ag}_2\text{Nb}_x$ BMGs with their critical diameters

Table 1 Thermal stability of $\text{Ti}_{47}\text{Cu}_{38-x}\text{Zr}_{7.5}\text{Fe}_{2.5}\text{Sn}_2\text{Si}_1\text{Ag}_2\text{Nb}_x$ glassy alloys

$x/\text{at}\%$	T_g/K	T_x/K	$\Delta T_x/\text{K}$
0	640	694	54
1	650	693	43
2	654	694	40

the three empirical compositional rules for achieving a high GFA and contribute to reducing the stability of the supercooled liquid. It was previously reported that repulsive interaction between the atomic pairs due to the positive mixing is thought to induce the formation of less dense random packed structures or atomic clusters, which leads to the easy nucleation and growth reactions of a crystalline phase, a lower viscosity and easier constituent element diffusion [20]. Therefore, the addition of Nb into Ti–Cu–Zr–Fe–Sn–Si–Ag BMG deteriorates the thermal stability and GFA.

The corrosion behaviors of $\text{Ti}_{47}\text{Cu}_{38}\text{Zr}_{7.5}\text{Fe}_{2.5}\text{Sn}_2\text{Si}_1\text{Ag}_2$ BMG in PBS solution were investigated in a former study [4]. To further understand the corrosion behaviors of the Ti–Cu–Zr–Fe–Sn–Si–Ag BMG in other artificial body fluids and the effect of Nb addition, a more complex Hank's solution which additionally contains Mg^{2+} , Ca^{2+} and glucose was adopted in this work. Figure 3a shows the changes in OCP with immersion time for the Ti-based BMGs in Hank's solution aerated with 4 vol% O_2/N_2 . For all alloys, the OCP values rise steeply with immersion time during the initial 50 s and then reach stationary values,

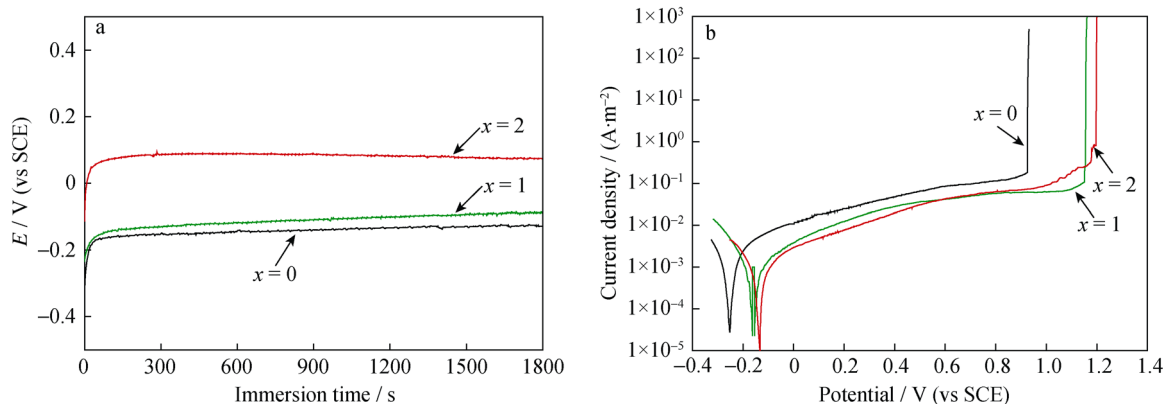


Fig. 3 Changes in open-circuit potentials (E) with immersion time **a** and potentiodynamic polarization curves **b** of $\text{Ti}_{47}\text{Cu}_{38-x}\text{Zr}_{7.5}\text{Fe}_{2.5}\text{Sn}_2\text{-Si}_1\text{Ag}_2\text{Nb}_x$ BMGs in Hank's solution at 310 K with 4 vol% O_2/N_2

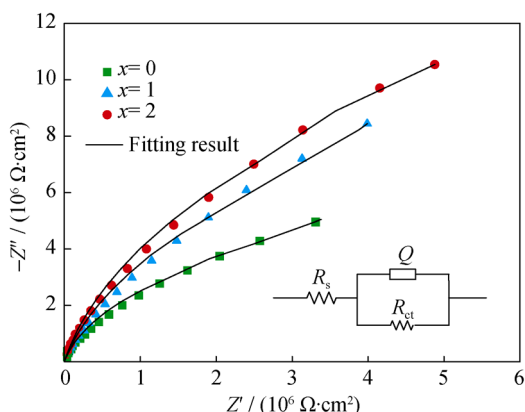


Fig. 4 Nyquist diagrams of experimental data and fitted curves of real part (Z') and imaginary part (Z'') of impedance and equivalent circuit used in EIS results of interpretation $R_s(R_{ct}Q)$ for $\text{Ti}_{47}\text{Cu}_{38-x}\text{Zr}_{7.5}\text{Fe}_{2.5}\text{Sn}_2\text{Si}_1\text{Ag}_2\text{Nb}_x$ BMGs in Hank's solution at 310 K

Table 2 Values of fitted parameters by equivalent circuit of $\text{Ti}_{47}\text{Cu}_{38-x}\text{Zr}_{7.5}\text{Fe}_{2.5}\text{Sn}_2\text{Si}_1\text{Ag}_2\text{Nb}_x$ glassy alloys in Hank's solution at 310 K with 4 vol% O_2/N_2 aeration

$x/\text{at}\%$	$R_s/(\Omega\cdot\text{cm}^2)$	$R_{ct}/(10^7\Omega\cdot\text{cm}^2)$	$Y_0/(10^{-6}\Omega^{-1}\cdot\text{cm}^{-2}\cdot\text{s}^{-n})$	n
0	66.54	1.119	1.496	0.9129
1	120.50	2.522	1.074	0.9126
2	77.39	3.367	1.047	0.9223

implying the formation of stable surface film during the immersion in Hank's solution. It can also be observed that the OCP value slightly increases with the addition of 1 at% Nb and then increases drastically up to about 0.08 V when Nb content reaches 2 at%. This result indicates that the stability of surface film on glassy alloys is enhanced with the increase in Nb content. Potentiodynamic polarization

curves of the glassy alloys in Hank's solution open to air at 310 K are shown in Fig. 3b. It can be seen that the Ti-based glassy alloys are spontaneously passivated with a wide passive region and low passive current densities around $0.1\text{ A}\cdot\text{m}^{-2}$, and pitting corrosion corresponding to the abrupt rise in the current density occurs at relatively high potential. With the Nb content of the Ti-based glassy alloys increasing from 0 at% to 2 at%, the passive current density becomes lower and the pitting potential remarkably increases from 0.90 to 1.21 V. The nobler OCP, higher pitting potential and lower passive current density of the Nb-bearing glassy alloys demonstrate that Nb addition is effective on improving the bio-corrosion resistance of the novel $\text{Ti}_{47}\text{Cu}_{38}\text{Zr}_{7.5}\text{Fe}_{2.5}\text{Sn}_2\text{Si}_1\text{Ag}_2$ BMG in Hank's solution [21], which is favorable for the biomedical applications.

Impedance spectra of $\text{Ti}_{47}\text{Cu}_{38-x}\text{Zr}_{7.5}\text{Fe}_{2.5}\text{Sn}_2\text{Si}_1\text{Ag}_2\text{Nb}_x$ glassy alloys are presented as the Nyquist diagram in Fig. 4. It is obvious that the Nyquist diagram of each alloy is characterized by depressed semicircle and only consists of a single capacitance loop. The diameter of the semicircle, depending on the resistance of the passive layer, increases with Nb content, which indicates the enhancement of the corrosion resistance [22]. The fitting curves were obtained using the $R_s(R_{ct}Q)$ model (inset in Fig. 4), where R_s denotes the solution resistance, R_{ct} denotes the charge transfer resistance which reflects the corrosion rate of a metal in solutions [23, 24], and Q denotes the constant phase element (CPE) instead of pure capacity given the deviations of the system from the ideality due to surface heterogeneities and other possible reasons [25]. The impedance of the CPE (Z_{CPE}) is defined by:

$$Z_{\text{CPE}} = Y_0^{-1}(j\omega)^{-n} \tag{1}$$

where j is imaginary part, ω is angular frequency, Y_0 is admittance constant, and n is the dispersion coefficient. When $n = 1$, the CPE is a capacitor, and when $n = 0$, the

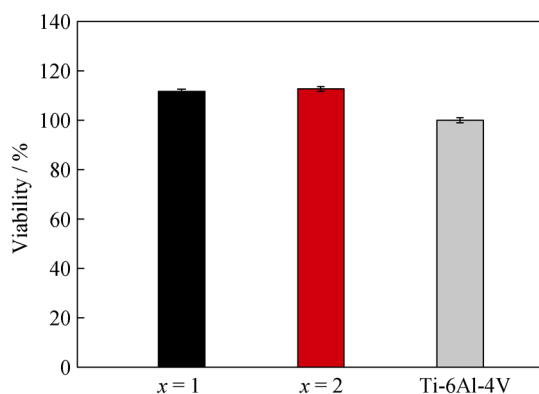


Fig. 5 Cytotoxicity of MC3T3-E1 cells cultured on $\text{Ti}_{47}\text{Cu}_{38-x}\text{Zr}_{7.5}\text{Fe}_{2.5}\text{Sn}_2\text{Si}_1\text{Ag}_2\text{Nb}_x$ BMGs and Ti-6Al-4V alloy for 24 h

CPE is a simple resistor. The fitting parameters of the equivalent circuit are listed in Table 2. It is apparent that the R_{ct} value of the Ti-based glassy alloys increases with Nb content increasing, which is in accordance with the higher pitting potential and lower passive current density resulted from the increase in Nb content as shown in Fig. 3b. It is suggested that Nb could be enriched in the surface oxide films on the Ti-based BMGs containing Nb and depress the diffusion of Cu, leading to the formation of more protective surface film and the higher bio-corrosion resistance [12].

The result of MTT assay for Ti-Cu-Zr-Fe-Sn-Si-Ag-Nb BMGs is illustrated in Fig. 5. It can be seen that the Nb-bearing Ti-based BMGs exhibit similar cell viabilities to Ti-6Al-4V alloy, and there is no significant variation in cell viabilities for BMGs with different Nb contents. Figure 6 shows the morphologies of MC3T3-E1 cells after cultivating on Ti-based BMGs and Ti-6Al-4V alloy for 24 h. Cells spread extensively on the alloys with polygonal and spindle shapes, and contact with each other through filopodia. This further confirms that the Nb-bearing Ti-based BMGs exhibit excellent in vitro biocompatibility compared with Ti-6Al-4V alloy. Good in vitro biocompatibility of Nb-bearing Ti-based BMGs may be attributed to the substitution of Cu with more biocompatible Nb element and the enhanced bio-corrosion resistance

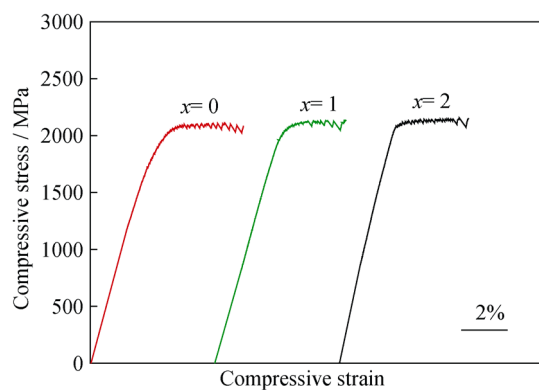


Fig. 7 Compressive stress-strain curves of $\text{Ti}_{47}\text{Cu}_{38-x}\text{Zr}_{7.5}\text{Fe}_{2.5}\text{Sn}_2\text{Si}_1\text{Ag}_2\text{Nb}_x$ BMGs

which further helps to mitigate the release of constituent elements of the BMGs to the physiological environment.

Figure 7 shows the compressive stress-strain curves of as-cast glassy alloy rods with diameter of 2 mm. All the Ti-based BMGs exhibit large elastic strain of about 2 % and subsequent plastic deformation prior to final fracture. Mechanical properties of these Ti-based BMGs are summarized in Table 3. It is seen that with the addition of Nb, there is no obvious change in compressive strength, plastic strain, Young's modulus as well as Vickers hardness, which are around 2000 MPa, 2 %, 98 GPa and HV 590, respectively. SEM observation indicates that the Ti-based BMGs exhibit similar fracture morphology, and the SEM images of the fractured $\text{Ti}_{47}\text{Cu}_{36}\text{Zr}_{7.5}\text{Fe}_{2.5}\text{Sn}_2\text{Si}_1\text{Ag}_2\text{Nb}_2$ BMG are shown in Fig. 8 as representatives. The fracture surface exhibits typical vein-like morphology (Fig. 8a), which is characteristic for ductile BMGs [26]. As shown in Fig. 8b, a number of primary shear bands parallel to the fracture plane and secondary shear bands are formed on the lateral surface of the fractured sample, which contributes to the plasticity of the Ti-based BMGs. Moreover, it is also noted that with Nb content in the Ti-based BMGs increasing from 0 at% to 2 at%, the ratio of Vickers hardness to Young's modulus (HV/E) increases from 0.059 to 0.061, which may facilitate good anti-wear performance [27, 28]. The high compressive strength, hardness and HV/

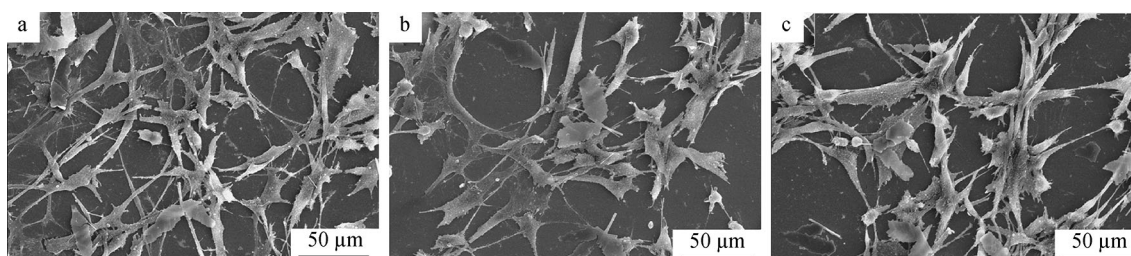
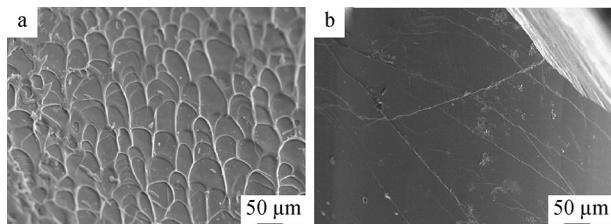


Fig. 6 SEM images of MC3T3-E1 cells on cast $\text{Ti}_{47}\text{Cu}_{38-x}\text{Zr}_{7.5}\text{Fe}_{2.5}\text{Sn}_2\text{Si}_1\text{Ag}_2\text{Nb}_x$ (a $x = 1$ and b $x = 2$) BMGs and c Ti-6Al-4V alloy after incubation for 24 h

Table 3 Mechanical properties of $Ti_{47}Cu_{38-x}Zr_{7.5}Fe_{2.5}Sn_2Si_1Ag_2Nb_x$ BMGs

$x/at\%$	σ_y/MPa	σ_f/MPa	$\varepsilon_p/\%$	E/GPa	HV	HV/ E
0	1972 ± 63	2031 ± 57	2.5 ± 0.2	100.4 ± 0.1	588 ± 6	0.059
1	1973 ± 53	2070 ± 43	1.9 ± 0.2	98.9 ± 0.2	590 ± 4	0.060
2	2010 ± 66	2078 ± 51	2.1 ± 0.2	97.1 ± 0.1	593 ± 4	0.061

σ_y , yielding strength; σ_f , fracture strength; ε_p , plastic strain; E , Young's modulus; HV, Vickers microhardness; HV/ E , ratio of HV to E

**Fig. 8** SEM images of $Ti_{47}Cu_{36}Zr_{7.5}Fe_{2.5}Sn_2Si_1Ag_2Nb_2$ BMG after compressive deformation: **a** fracture and **b** lateral surfaces

E values combined with relatively low Young's modulus of the Nb-bearing Ti-based BMGs suggest better mechano-compatibility as biomaterials.

4 Conclusion

$Ti_{47}Cu_{38-x}Zr_{7.5}Fe_{2.5}Sn_2Si_1Ag_2Nb_x$ ($x = 0, 1, 2; at\%$) BMGs with critical diameters up to 3 mm were developed, though the minor addition of Nb to the Ti–Cu–Zr–Fe–Sn–Si BMG is slightly detrimental to the glass-forming ability. With the increase in Nb content from 0 at% to 2 at% in Ti–Cu–Zr–Fe–Sn–Si–Ag–Nb BMGs, the bio-corrosion resistance in Hank's solution is enhanced, which is indicated by the nobler OCP, higher pitting potential, lower passive current density and larger charge transfer resistance. The improved bio-corrosion resistance with the Nb-alloying is attributed to the formation of more protective surface film, as evidenced by EIS measurement. Excellent biocompatibility of Nb-bearing Ti-based BMGs is revealed by the MTT assay results and cell behaviors. The Nb addition to the Ti-based BMG has no apparent effect on mechanical properties. The combination of enhanced bio-corrosion resistance, good biocompatibility and mechanical properties demonstrates the potential of Ti-based BMGs for use in biomedical applications.

Acknowledgments This work was financially supported by the National Natural Science Foundation of China (Nos. 51161130526 and 51271008).

References

- [1] Xie GQ, Qin FX, Zhu SL. Recent progress in Ti-based metallic glasses for application as biomaterials. *Mater Trans.* 2013;54(8):1314.
- [2] Zhu SL, Wang XM, Qin FX, Inoue A. A new Ti-based bulk glassy alloy with potential for biomedical application. *Mater Sci Eng, A.* 2007;459(1–2):233.
- [3] Zhu SL, Xie GQ, Qin FX, Wang XM, Inoue A. Effect of minor Sn additions on the formation and properties of TiZrCuPd bulk glassy alloy. *Mater Trans.* 2008;53(3):500.
- [4] Pang SJ, Liu Y, Li HF, Sun LL, Li Y, Zhang T. New Ti-based Ti–Cu–Zr–Fe–Sn–Si–Ag bulk metallic glass for biomedical applications. *J Alloys Compd.* 2015;625:323.
- [5] Oak JJ, Louzguine-Luzgin DV, Inoue A. Investigation of glass-forming ability, deformation and corrosion behavior of Ni-free Ti-based BMG alloys designed for application as dental implants. *Mater Sci Eng, C.* 2009;29(1):322.
- [6] Fornel J, Pellicer E, Van Steenberge N, Gonzalez S, Gebert A. Improved plasticity and corrosion behavior in Ti–Zr–Cu–Pd metallic glass with minor additions of Nb: an alloy composition intended for biomedical application. *Mater Sci Eng, A.* 2013; 559(1):159.
- [7] Calin M, Gebert A, Ghinea AC, Gostin PF, Abdi S, Mickel C, Eckert J. Designing biocompatible Ti-based metallic glasses for implant applications. *Mater Sci Eng, A.* 2013;33(2):875.
- [8] Oak JJ, Inoue A. Attempt to develop Ti-based amorphous alloys for biomaterials. *Mater Sci Eng, A.* 2006;449–451:220.
- [9] Oak JJ, Louzguine-Luzgin DV, Inoue A. Fabrication of Ni-free Ti-based bulk metallic glassy alloy having potential for application as biomaterial, and investigation of its mechanical properties, corrosion, and crystallization behavior. *J Mater Res.* 2007;22(5): 1346.
- [10] Hanawa T. Evaluation techniques of metallic biomaterials in vitro. *Sci Technol Adv Mater.* 2002;3(4):289.
- [11] Tavares AMG, Fernandes BS, Souza SA, Batista WW, Cunha FGC, Landders R, Macedo MCSS. The addition of Si to the Ti–35Nb alloy and its effect on the corrosion resistance when applied to biomedical materials. *J Alloys Compd.* 2014;591(4): 91.
- [12] Pang SJ, Zhang T, Asami K, Inoue A. Formation, corrosion behavior, and mechanical properties of bulk glassy Zr–Al–Co–Nb alloys. *J Mater Res.* 2003;18(7):1652.
- [13] Pang SJ, Zhang T, Kimura H, Asami K, Inoue A. Corrosion behavior of Zr–(Nb–)Al–Ni–Cu glassy alloys. *Mater Trans, JIM.* 2000;41(11):1490.
- [14] Lu XY, Huang L, Pang SJ. Formation and biocorrosion behavior of Zr–Al–Co–Nb bulk metallic glasses. *Chin Sci Bull.* 2012;14(14):1723.
- [15] Fornel J, Pellicer E, Van Steenberg N, Gonzalez S, Gebert A, Surinach S, Baro MD, Sort J. Improved plasticity and corrosion behavior in Ti–Zr–Cu–Pd metallic glass with minor additions of

- Nb: an alloy composition intended for biomedical applications. *Mater Sci Eng, A*. 2013;559(3):159.
- [16] Tam MK, Pang SJ, Shek CH. Corrosion behavior and glass-forming ability of Cu–Zr–Al–Nb alloys. *J Non-Cryst Solids*. 2007;353(32–40):3596.
- [17] Asami K, Qin CL, Zhang T, Inoue A. Effect of additional elements on the corrosion behavior of Cu–Zr–Ti bulk metallic glass. *Mater Sci Eng, A*. 2004;375–377:235.
- [18] Wang WH. The elastic properties, elastic models and elastic perspectives of metallic glasses. *Prog Mater Sci*. 2012;57(3):487.
- [19] Takeuchi A, Inoue A. Classification of bulk metallic glasses by atomic size difference, heat of mixing and period of constituent elements and its application to characterization of the main alloying element. *Mater Trans*. 2005;46(12):2817.
- [20] Inoue A, Shibata T, Zhang T. Effect of additional elements on glass transition behavior and glass formation tendency of Zr–Al–Cu–Ni alloys. *Mater Trans, JIM*. 1995;36(12):1420.
- [21] Li Y, Zhang F, Zhao TT, Tang M, Liu Y. Enhanced wear resistance of NiTi alloy by surface modification with Nb ion implantation. *Rare Met*. 2014;33(3):244.
- [22] Huang YZ, Blackwood DJ. Characterisation of titanium oxide film grown in 0.9% NaCl at different sweep rates. *Electrochim Acta*. 2005;51(6):1099.
- [23] Ma HY, Chen SH, Yin BS, Zhao SY, Liu XQ. Impedance spectroscopic study of corrosion inhibition of copper by surfactants in the acidic solutions. *Corros Sci*. 2003;45(5):867.
- [24] Valdez B, Kiyota S, Stoytcheva M, Zlatev R, Bastidas JM. Cerium-based conversion coatings to improve the corrosion resistance of aluminium alloy 6061-T6. *Corros Sci*. 2014;87(5):141.
- [25] Altube A, Oierna AR. Thermal and electrochemical properties of cobalt containing finemet type alloys. *Electrochim Acta*. 2004;49(2):303.
- [26] Li DK, Zhang HF, Wang AM, Zhu ZW, Hu ZQ. Effect of Sn addition on the glass-forming ability and mechanical properties of Ni–Nb–Zr bulk metallic glasses. *Chin Sci Bull*. 2011;56(36):3926.
- [27] Huang L, Cao Z, Meyer HM, Liaw PK, Garlea E, Dunlap JR, Zhang T, He W. Responses of bone-forming cells on pre-immersed Zr-based bulk metallic glasses: effects of composition and roughness. *Acta Biomater*. 2011;7(1):395.
- [28] Leyladn A, Matthews A. Design criteria for wear-resistant nanostructured and glassy-metal coatings. *Surf Coat Technol*. 2004;177–178:317.